CA9700774

PREDICTION OF PRESSURE TUBE FRETTING-WEAR DAMAGE DUE TO FUEL VIBRATION

M.YETISIR and N.J. FISHER

AECL
VIBRATION AND TRIBOLOGY UNIT
Fluid Sealing and Dynamics Branch
Engineering Technologies Division
Chalk River Laboratories
Chalk River, Ontario Canada K0J 1J0

ABSTRACT

Fretting marks between fuel bundle bearing pads and pressure tubes have been observed at the inlet end of some Darlington NGS and Bruce NGS fuel channels. The excitation mechanisms that lead to fretting are not fully understood. In this paper, the possibility of bearing pad-to-pressure tube fretting due to turbulence-induced motion of the fuel element is investigated. Numerical simulations indicate that this mechanism by itself is not likely to cause the level of fretting experienced in Darlington and Bruce NGS's.

1. INTRODUCTION

Fuel damage discovered during the 1990 November refueling of Darlington Nuclear Generating Station (NGS) resulted in an investigation that identified acoustic pressure fluctuations as the cause of end plate cracking. During the investigation, it was also found that, at the inlet, both the pressure tube and the fuel bundle bearing pads had experienced high levels of fretting damage. Further investigation revealed similar fretting patterns in other fuel channels in Darlington and Bruce NGS's.

The purpose of this study was to numerically investigate a postulated excitation mechanism (i.e., fuel element turbulence excitation) to assess the likelihood that it is responsible for the large pressure tube-to-bearing pad fretting rates observed in Darlington and Bruce NGS's.

2. FRETTING DAMAGE PREDICTION

2.1 General Approach

Fretting damage is quantified in terms of the removed volume of fretted material. The rate of volume removal, $\dot{V}$, is related to the normal work-rate, $\dot{W}_N$, through Archard's wear model (Suh, 1986) as given below:

$$\dot{V} = K\dot{W}_N \tag{1}$$

where, $\dot{V}$: Volume wear rate (m^3/s)
K : Empirical wear coefficient (1/Pa)

$\dot{W}_N = \frac{1}{\Delta t}\int_{\Delta t} F_N ds$: Pressure tube-to-bearing pad normal work-rate (W)

F_N : Normal force (N)
s : Sliding displacement (m)
t : Time (seconds)

The wear coefficient, K, is obtained experimentally for a particular material combination and operating conditions. The normal work-rate, $\dot{W}_N$, is computed by the finite element program, VIBIC. The rate of volume removal due to fretting can then be predicted from Equation 1.

2.2 Fuel Bundle Bearing Pad-to-Pressure Tube Fretting

Considerable fretting testing of fuel element bearing pads interacting with sections of pressure tube has been conducted over the past four years. In terms of wear coefficients, the fundamental fretting data indicate that reasonable values of the zirconium wear coefficients are 50 to 200 x 10^{-15} Pa^{-1} at low temperatures (<100°C) and fuel channel outlet temperatures (315°C), and 500 to 2500 x 10^{-15} Pa^{-1} at inlet temperatures (265°C). The ranges in these wear coefficients indicate the measurement uncertainties.

Based on the field data and with the assumption that the in-reactor damage occurred over the full bearing pad surface (2.7mm x 25.4 mm) during a bundle residency of 120 days, the upper decile value of the wear-rate is found to be 1 μm/day. For wear coefficient values of 500 to 2500 x 10^{-15} Pa^{-1}, work-rates of 0.3 to 1.6 mW would be required to cause a fretting rate of 1 μm/day.

2.3 Definition of Gap and Preload

The terms "gap" and "preload" are frequently used in this paper. The term "gap" indicates that, when the fuel bundle and the modelled fuel element are stationary, the pressure tube and the fuel element are not in contact. A 20 μm gap means that the fuel element surface is 20 μm from the pressure tube and zero gap means that the fuel element is just touching the pressure tube when there is no excitation force. If the fuel element is moved towards the pressure tube from the zero gap position, a static contact force develops due to bending of the fuel element. This force is called the "preload". By definition, at zero gap, the preload is also zero. Hence, the zero gap case is called "0 gap/preload" in this paper to indicate that the preload is also zero.

3. FUEL ELEMENT VIBRATION - NUMERICAL SIMULATIONS

3.1 Fuel Element Model

The VIBIC (VIbration of Beams with Intermittent Contact) finite element program was originally designed for modelling heat exchanger tubes with circular clearance supports. The VIBIC model of a fuel element is shown Figure 1, where the clearance support is the pressure tube. The geometric and material properties of the fuel element were obtained from various references and are tabulated in Table 1. As shown in Figure 1, translational motion at both ends of the fuel element was restricted. End plate bending stiffness was modelled with rotational springs about the y- and z-axes. The stiffness value of these springs, computed from the stiffness of the fuel bundle end plates, was 40 N·m/rad.

The ovalization stiffnesses of the fuel element/bearing pad and the pressure tube were represented by an equivalent linear spring in the radial direction. This equivalent contact stiffness, $k_{contact}$, is the combined stiffness of the fuel element/bearing pad and the pressure tube local ovalization stiffnesses. This stiffness is evaluated as the sum of the fuel element/bearing pad, $k_{fe/bp}$, and pressure tube, k_{pt}, local stiffnesses in series:

$$k_{contact} = \left[\frac{1}{k_{fel\,bp}} + \frac{1}{k_{pt}} \right]^{-1} \tag{2}$$

The local stiffnesses can be evaluated using expressions derived by Morley (1960) and Lukasewizc (1979). The fuel element local stiffness, assuming no contribution from the bearing pad, is in the order of 0.5 to 1.2 N/μm. The pressure tube local stiffness is greater, in the order of 4 to 12 N/μm. Therefore, the equivalent contact stiffness is in the range of 1 to 10 N/μm, but closer to 1 than 10 N/μm.

3.2 Modal Analysis

The fuel element was discretized into 30 equal-length finite elements. Translational and rotational motions in the x-direction were not included in the analysis, since the main focus of this study was to investigate transverse vibration of fuel elements or bundles.

Calculated modal frequencies are listed in Table 2 and the mode shapes for the first three modes are shown in Figure 2. These mode shapes are typical of a continuous beam with hinged end supports. The small effect of the end support plates is seen in the first mode shape, where the maximum slope is not at the end points, but at about one-tenth of the element length from the end points. The first mode natural frequency of 31.98 Hz is very close to that from previous experimental measurements with a single fuel element (at 5.5 MPa non-flowing water the natural frequency was measured as 31.7 Hz).

3.3 VIBIC: A Special Purpose Non-linear Finite Element Program

The VIBIC computer code is a finite element model of a multi-span beam (tube). It includes the effect of non-linearities due to clearances between the beam and its supports. The code simulates the beam response to external sinusoidal or random force excitation and predicts beam motion and dynamic interaction at the supports.

The code structure and organization have been described in detail in previous publications (Rogers and Pick, 1976 and 1977; and Ko and Rogers, 1981). The code embodies state-of-the-art flow-induced vibration and fretting technology and has been extensively tested against experimental measurements, benchmark solutions and other finite element code results (Ko and Rogers, 1981; Fisher et al., 1989; and Fisher and Weckwerth, 1990).

3.4 Random (Turbulence) Excitation

Turbulence excitation was modelled using a series of random numbers with appropriate frequency content and RMS value.

3.4.1 Forcing Function

To model random turbulence excitation, six uncorrelated random excitation forces were applied uniformly along the fuel element in both the y- and z-directions. At each of the six nodes where the forces were applied, the forces in each direction (y- and z-directions) were uncorrelated, but of equal RMS magnitude. Each force was generated as white noise in the frequency spectrum, and then filtered by a third-order Butterworth filter with 70 Hz cut-off frequency to result in a frequency content typical of random turbulence excitation due to fluid axial flow (Gorman, 1975).

The simulation time for a typical VIBIC simulation with turbulence excitation was 4.2 seconds, resulting in the typical force spectrum shown in Figure 3. Since there are six points of force excitation along the length of the fuel element, the turbulence correlation length is implicitly one-sixth of the fuel element length.

3.4.2 Reference Case

For the random turbulence excitation reference, the excitation forces were scaled so that the total displacement at the mid-point of the fuel element was 100 μm RMS in the absence of bearing pad-to-pressure tube contact. The required level of excitation for that displacement was 0.16 N RMS for each force. For the 0 gap/preload case, the resulting work-rate was 0.93 mW.

3.4.3 Simulation Time

With random excitation, statistical parameters, like RMS contact force, RMS displacement and work-rate, changed significantly from one cycle (in VIBIC, a cycle is a time period specified by the user through aggregate cycles) to another. However, the averaged values do not vary significantly after 3.0 seconds of simulation time. Since, with random excitation runs, computation time and data storage become prohibitive, it was decided that a 4.2 second simulation time be used for all simulations.

3.4.4 Effect of Random Numbers

Due to randomness, fuel element motion for the same level of excitation but different sets of random numbers is different. However, the variation in average results due to using different sets of random numbers should diminish as the simulation time approaches infinity. The variation in predicted work-rate for four different sets of random numbers is shown in Figure 4. After 4.2 seconds of simulation time, the difference between two runs is about 20%. Simulations of a simplified system conducted for 220 seconds simulation time resulted in differences of 10% in work-rate. As the additional computational effort required to achieve this improvement in convergence was great for this simplified system, longer simulations were not considered worthwhile. Instead, when necessary, the same simulation case was repeated with different sets of random numbers to obtain average results.

3.4.5 Effect of Contact Stiffness

Series of runs were conducted for the 0 gap/preload and 0.5 N preload cases at the greatest excitation level. Work-rate is not significantly affected when the contact stiffness is varied over several orders of magnitude. This is due to the relative magnitudes of fuel element bending stiffness and the local contact stiffness. The fuel element bending stiffness[1] is 1.4×10^5 N/m. When $k_{contact} \geq 1.4 \times 10^5$ N/m, the impact dynamics are dominated by the fuel element bending stiffness. This effect can be clarified by considering the fuel element and contact stiffness as two springs in series, where the spring with smaller stiffness dominates the dynamics. Therefore, work-rate is rather insensitive to contact stiffness when $k_{contact} \geq 1.4 \times 10^5$ N/m. The variation in work-rate is 22% over a contact stiffness range of 10^5 to 10^8 N/m. Similar results have been obtained by other researchers (Rogers and Pick, 1976; and Yetisir and Weaver, 1986).

The important conclusion from these results is that, even if the computed (and modelled) contact stiffness is in error by a factor of two or more, the results and trends presented in this paper are still valid.

3.4.6 Effect of Friction Coefficient

The effect of friction coefficient was investigated using friction coefficients of 0.3, 0.5 (the reference value) and 0.7. Figures 5(a) and (b) show normal work-rates for the 0 gap/preload and 0.5 N preload cases as functions of friction coefficient. Work-rate varies significantly with friction coefficient. This can be explained by considering the vibration frequency of these cases. With sinusoidal excitation, the fuel element vibrates at the excitation frequency, which was 25 Hz. With random excitation, the fuel element vibrates at its natural frequency. Vibration amplitude at the natural frequency is inversely proportional to the square root of damping. Therefore, if the friction

---

1 . The bending stiffness used in VIBIC is equal to $k = F/\delta$ where δ is the beam-like deflection of the fuel element at the contact location due to the normal load F at the same point (with no pressure tube contact).

mechanism at the contact is considered to be a damping mechanism, sliding distance and, hence work-rate, should be sensitive to changes in coefficient of friction.

Previous experimental measurements by Fisher et al. indicate that the friction coefficient is not likely to be less than 0.5. Therefore, the value of 0.5 used for the reference case represents a conservative value, as it yields higher work-rates than the value of 0.7.

3.4.7 Effect of Damping

Figure 6 shows the effect of modal damping on work-rate. Increasing damping decreases work-rate. This result is expected since vibration amplitude in both the normal and sliding directions decreases with increasing damping. As a result, both contact force and sliding distance are reduced, resulting in reduced work-rate.

3.4.8 Effect of Bundle Length

The effect of bundle length was investigated to assess the effect of new 2.5% longer fuel bundles on fretting. Because the variation in work-rate due to randomness might overshadow the variation due to change in length if only 2.5% longer bundles were considered, 5 and 10% longer fuel bundles were modelled and the results were extrapolated to determine the effect for 2.5% longer fuel bundles. Figure 7 shows the results for a standard bundle (0.495 m in length), 5% longer bundle and 10% longer bundle for five sets of random numbers. For these runs, excitation force per unit length was kept constant. The same sets of random numbers were used for all bundle lengths for consistency.

Results show that work-rate increases with increasing bundle length. The reason for this increase is that longer bundles are more flexible, resulting in larger vibration amplitudes when the force per unit length is kept constant. On average, 5 and 10% longer bundles have 9 and 15% larger work-rates. Extrapolation of the results indicates that the 2.5% longer fuel bundle would experience about 5% more fretting than the standard bundle if all other parameters, such as damping, friction coefficient, etc., remain unchanged.

3.4.9 Effect of Element Stiffness

Fuel elements become stiffer with power in-reactor due to irradiation. To investigate the effect of element stiffening, a series of runs was conducted. The results are plotted in Figure 8. Increased stiffness of the element was simulated by increasing the value of the elastic modulus, E. The excitation level was held constant for the stiffer element model. Doubling the value of the stiffness reduced the work-rate by 25%.

3.4.10 Effect of Gap/Preload

The gap between the fuel element and the pressure tube was varied by moving the equilibrium position of the fuel element with respect to the pressure tube. A series of runs was performed using three levels of excitation forces (0.16, 0.08 and 0.04 N RMS) for various gap and preload cases. These excitation levels correspond to 100, 50 and 25 μm total RMS displacements, respectively, when there is no bearing pad-to-pressure tube contact. Results are shown in Figure 9. The relationship between work-rate and excitation force level (or wear depth rate and free displacement (no contact)) is a power relationship. An increase in free displacement by a factor of four (from 25 to 100 μm RMS) results in an increase in work-rate by a factor of 15 at 0 gap/preload.

For all three excitation levels, maximum work-rate occurs at low preloads. Work-rates are reduced with increasing preload because of decreased sliding distances. At preloads larger than 2.0, 1.0 and 0.5 N for the excitation levels of 0.16, 0.08 and 0.04 N RMS, respectively, sliding distances become so small (smaller than 5 μm) that the bearing pad is considered to be stuck to the pressure tube. When sticking occurs, fretting rates reduce practically to zero.

Note that the 0.04 N RMS excitation force is considered to be the most realistic excitation level as it results in 25 μm total RMS displacement at the mid-point of the fuel element. However, with this excitation level, the

maximum predicted work-rate is only 0.058 mW. This is significantly lower than the 0.3 to 1.6 mW work-rate that is required to cause fretting rates of 1 μm/day.

3.4.11 Fretting Damage

Pressure tube wear depth is shown versus bundle residence time in Figure 10 for three levels of excitation force. These curves are obtained using a typical wear coefficient for inlet channel conditions, 1000×10^{-15} Pa^{-1}. With this value of wear coefficient, a work-rate of 0.8 mW corresponds to a wear depth rate of 1 μm/day, if the wear is assumed to occur evenly over the full surface of a bearing pad of 2.7 mm width and 25.4 mm length.

Two curves are shown for each level of excitation. The initial contact condition assumed for both curves was 0 gap/preload. To generate the linear curve (straight line), the initial contact condition was maintained (i.e., the bearing pad was assumed to remain at the 0 gap/preload position). For this case to occur in-reactor, some mechanism, such as creep, must act to move the fuel element/bearing pad with time to maintain zero gap as the pressure tube and bearing pad wear. To generate the second curve, the fuel element/bearing pad was assumed to remain in the same position as it and the pressure tube wear, such that the gap increases with time and bearing pad-to-pressure tube interaction, and hence fretting, decreases. For this case the bearing pad was assumed to wear at one-half the rate of the pressure tube. These two curves likely bound in-reactor conditions. At the realistic level of interaction (25 μm RMS free vibration amplitude), fret marks of approximately 7 μm average depth would develop after 100 days of residence in the inlet position.

4. EXPERIMENTAL STUDY

The results of the computer simulations were somewhat surprising. It was of particular interest that low preloads of only a few Newtons magnitude were predicted to be sufficient to suppress bearing pad-to-pressure tube relative motion. Therefore, an experimental program was initiated to measure contact forces and relative displacements between a vibrating fuel element bearing pad and a section of pressure tube, compute work-rates, and compare these to those predicted in the numerical study.

The test set-up consisted of an element from a typical 37-element fuel bundle mounted inside a short length of pressure tube, as shown in Figure 11 and in contact with a work-rate measuring station (WORMS). The measuring station consisted of a small pressure tube specimen mounted on a Kistler Model 9251A piezoelectric triaxial load washer and instrumented with two Kaman Model KDM-7200-.5U miniature eddy-current displacement probes for measuring element displacement. The station was clamped to the outside of the pressure tube and access to the midplane bearing pad on the fuel element was achieved via a hole machined in the tube. The vertical position of the pressure tube specimen relative to the fuel element bearing pad was controlled to ±1 μm with a micrometer stage. O-ring seals between the measuring station and pressure tube permitted operation with water in the pressure tube. The fuel element was supported at the weld point of the two neighbouring elements of the outer ring.

Two Ling Model 102 electromechanical vibrators were flexibly mounted at the quarter-point of the element at 45° to the vertical. The vibrators were independently driven by filtered random sources to supply broadband random force excitation between 10 and 70 Hz frequency. Two PCB Model 208B piezoelectric force transducers were installed between the flexible links and the fuel element to monitor the excitation forces and ensure that they remained constant. The element was supported in a fixed rotary position, such that the bearing pad remained facing downwards toward the measuring station.

Measured and predicted work-rates for all three levels of excitation are plotted versus gap/preload in Fig. 9. The measured work-rate for each condition is the arithmetic average of the three four-second acquisitions. Error bars indicate the difference between the three acquisitions at some conditions.

The measured work-rates are in remarkably good agreement with the predictions. The relationship between gap/preload and work-rate was accurately predicted, with peak work-rates occurring at zero gap or at small

preloads. The peak measured work-rates were approximately 50 percent greater than predicted. Most importantly, the relative magnitude of the work-rates at each level of excitation are in good agreement. Therefore, the measurements confirm the prediction that fuel element vibration at typical values due to flow-induced random turbulence excitation is insufficient to cause the rates of fretting damage observed in-reactor.

5. SUMMARY AND CONCLUSIONS

Numerical investigations were conducted to study the effect of turbulence excitation on fretting-wear damage between fuel bundle bearing pads and pressure tubes. A parametric study was performed with the following constraints:

- Excitation forces were scaled such that the no-contact displacement at the mid-point was 25, 50 or 100 μm RMS.
- Bearing pad-to-pressure tube contact occurred at the mid-point.
- The pressure tube was stationary.

The following results were obtained:

- Maximum work-rates occur at low preloads (0.5 to 1.0 N) for all excitation levels.
- The effect of contact stiffness on work-rate is negligible.
- Work-rates decrease with increasing coefficient of friction and increasing modal damping.
- Longer fuel elements result in slightly greater damage if the excitation per unit length is kept constant. A 5% increase in element length resulted in a 9% increase in work-rate.
- Stiffer elements should experience less damage. A two-fold increase in stiffness should result in 25% less damage.

These results show that the fuel element vibration due to random turbulence cannot produce the 0.3 to 1.6 mW work-rate that is required to cause the 1 μm/day fretting rate observed in some in-reactor fuel channels. This conclusion is based on the assumptions that free vibration displacement was 25 μm RMS and that the wear coefficient was 500 to 2500 x 10^{-15} Pa^{-1}.

Experimental work was performed to verify the numerical simulations. It should be noted that all numerical results presented in this paper were obtained and reported before the design of the experimental setup and therefore are free of any bias and fine-tuning of parameters. The test results confirm the earlier predictions that fuel element vibration due to flow-induced random turbulence excitation is insufficient by itself to cause the rates of fretting damage observed in-reactor. Measured preloads to suppress bearing pad-to-pressure tube relative motion and measured work-rates at various gaps and preloads are in good agreement with predictions for all three levels of excitation.

6. ACKNOWLEDGEMENTS

The authors thank G. Field, , E. KØhn, A.G. Norsworthy, A. Maysner, C. Packer, R. Lalonde and related station operators for their input and support to this project. The valuable contributions of B. Smith and M.J. Pettigrew are greatfully acknowledged. This work is funded by CANDU Owners Group R&D work package WPIR 0137.

7. REFERENCES

Eisenger, F.L., Rao, M.S.M., Steininger, D.A., Haslinger, K.H., "Numerical Simulation of Fluidelastic Vibration and Comparison with Experimental Results", PVP - Vol. 206, Flow-Induced Vibration and Wear, ASME 1991.

Fisher, N.J., Olesen, M.J., Rogers, R.J. and Ko, P.L., "Simulation of Tube-to-Support Dynamic Interaction in Heat Exchange Equipment", Journal of Pressure Vessel Technology, Vol. 111, pp. 378-384, 1989.

Gorman, D.J., "Experimental and Anlaytical Study of Liquid and Two-Phase Flow-Induced Vibration in Reactor Fuel Bundles", 75-PVP-52, ASME Pressure Vessel and Piping Congress, 1975.

Maxwell, R.B., "Zirconium Alloys - Part 1: Physical Properties", CRNL Engineering Manual, (AECL Proprietary), Section 5 Materials, Subsection 3, 1969.

Morley, L.S.D., "The Thin-Walled Circular Cylinder Subjected to Concentrated Radial Loads", Quarterly Journal of Mechanics and Applied Mathematics, Vol XIII, Part 1, pp. 24-37, 1960.

Reynolds, W.C. and Perkins, H.C., Engineering Thermodynamics, Second Edition, McGraw-Hill, New York, 1977.

Rogers, R.J. and Pick, R.J., "On the Dynamic Spatial Response of a Heat Exchanger Tube with Intermittent Baffle Contacts", Nuclear Engineering and Design, Vol. 36, No. 1, pp. 81-90, 1976.

Rogers, R.J. and Pick, R.J., "Factors Associated with Support Plate Forces due to Heat Exchanger Tube Vibratory Contact", Nuclear Engineering and Design, Vol. 44, No. 2, pp. 247-253, 1977.

Rosinger, H.E. and Northwood, D.O., "The Elastic Properties of Zirconium Alloy Fuel Cladding and Pressure Tubing Materials", Journal of Nuclear Materials, Vol. 79, No. 1, pp. 170-179, 1979.

Suh, N.P., Tribophysics, Prentice-Hall Inc., Englewood Cliffs, New Jersey, 1986.

Vingsbo, O. and Soderberg, S., "On Fretting Maps", Wear of Materials, Vol. 2, pp. 885-894, 1987.

Yetisir, M. and Weaver, D.S., "The Dynamics of Heat Exchanger U-Bend Tubes with Flat Bar Supports", Journal of Pressure Vessel Technology, Vol. 108, pp. 406-413, 1986.

GEOMETRIC PROPERTIES	
Length	L = 495 mm
Outside Diameter of the Fuel Element	d_o = 13.1 mm
Inside Diameter of the Fuel Element	d_i = 12.2 mm
Inside Diameter of the Pressure Tube	rp = 51.5 mm

MATERIAL PROPERTIES	
Modulus of Elasticity @ 265 °C	E = 80.0 GPa
Poisson's Ratio @ 265 °C	υ = 0.35
Density of the Tube Material	ρ_{tube} = 6500 kg/m^3
Density of the Internal Element (UO2)	ρ_i = 10500 kg/m^3
Density of the Surrounding Fluid	ρ_f = 775 kg/m^3
Modal Damping Ratio @265 °C	ζ = 3.0 %

CONTACT PROPERTIES	
Contact Stiffness	$k_{contact}$ = 106 N/m
Contact Damping Coefficient	γ = 0.3 s/m
Coefficient of Friction	f = 0.5

BOUNDARY CONDITIONS		
Degrees of Freedom	**Nodes Affected**	**Condition**
x, θ_x	All Nodes	Restricted
y, z	End Nodes	Restricted
θ_y , θ_z	End Nodes	40 N·m/rad spring applied

TABLE 1: Properties of the Fuel Element as Used in the VIBIC Model

Mode #	Frequency [Hz]
1	31.98
2	116.8
3	255.8
4	445.2
5	681.9
6	959.1
7	1274
8	1617
9	1987
10	2373
11	2775
12	3181
13	3596
14	4004
15	4413

TABLE 2: Natural Frequencies of the Fuel Element with Rotational End Springs (End Points are Hinged and Subject to 40 N·m/rad Bending Springs

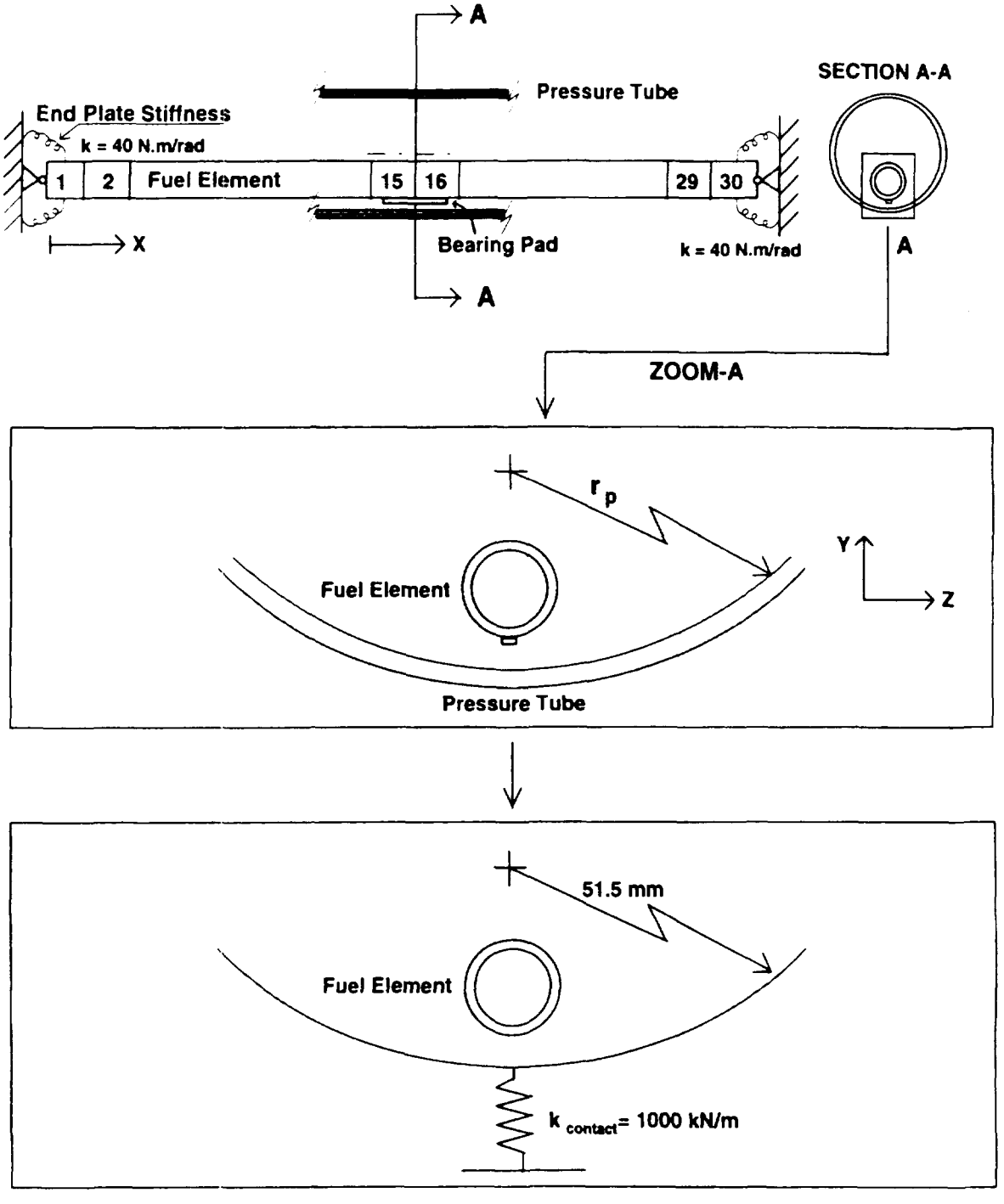

Figure 1: The VIBIC Model of Bearing Pad-to-Pressure Tube Contact

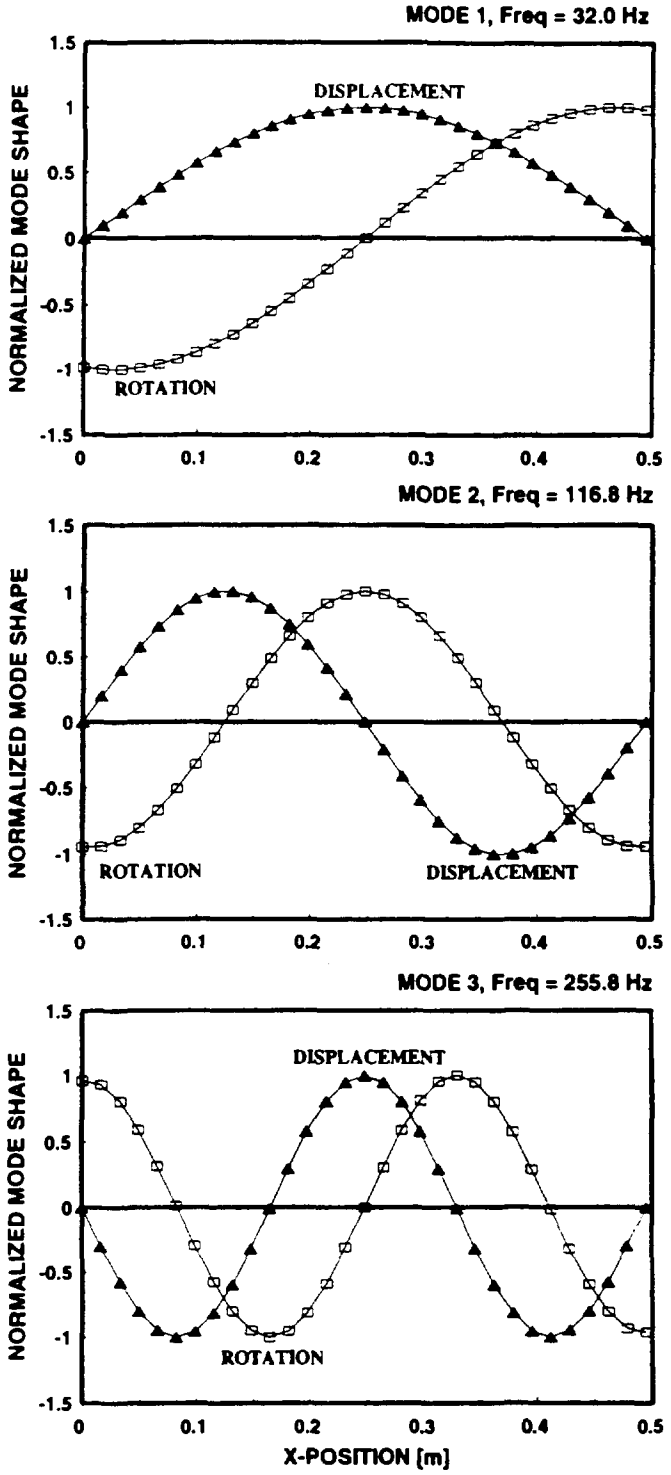

Figure 2: Lowest Three Mode Shapes of the Fuel Element with End Support Plates

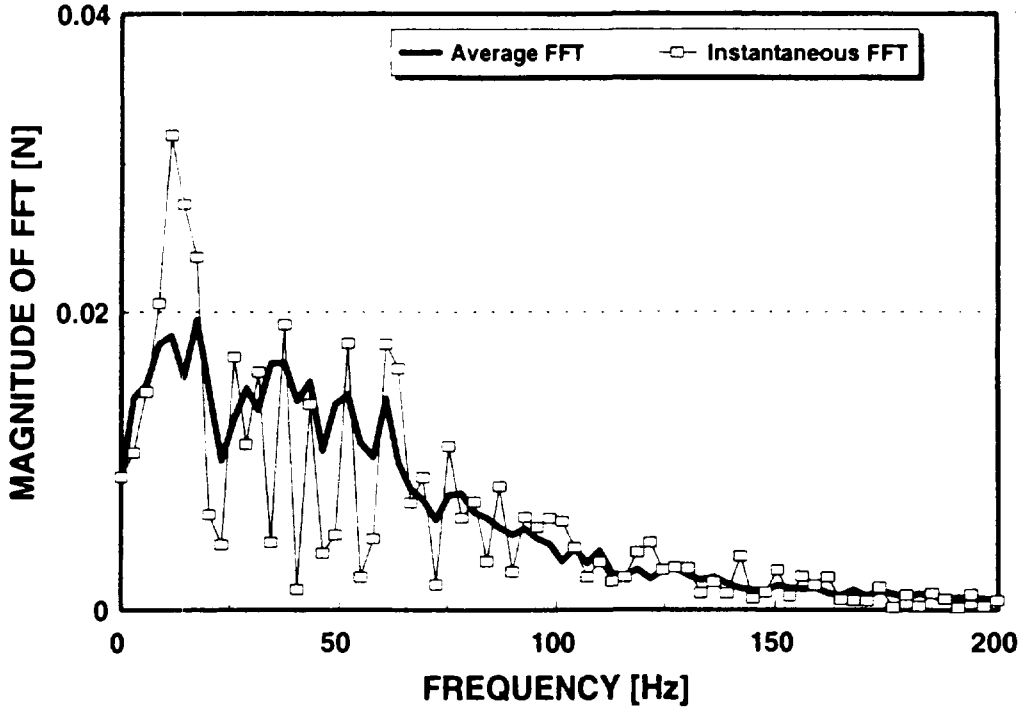

Figure 3: Frequency Content of a Turbulence Excitation Force for 5 Seconds of Simulation Time

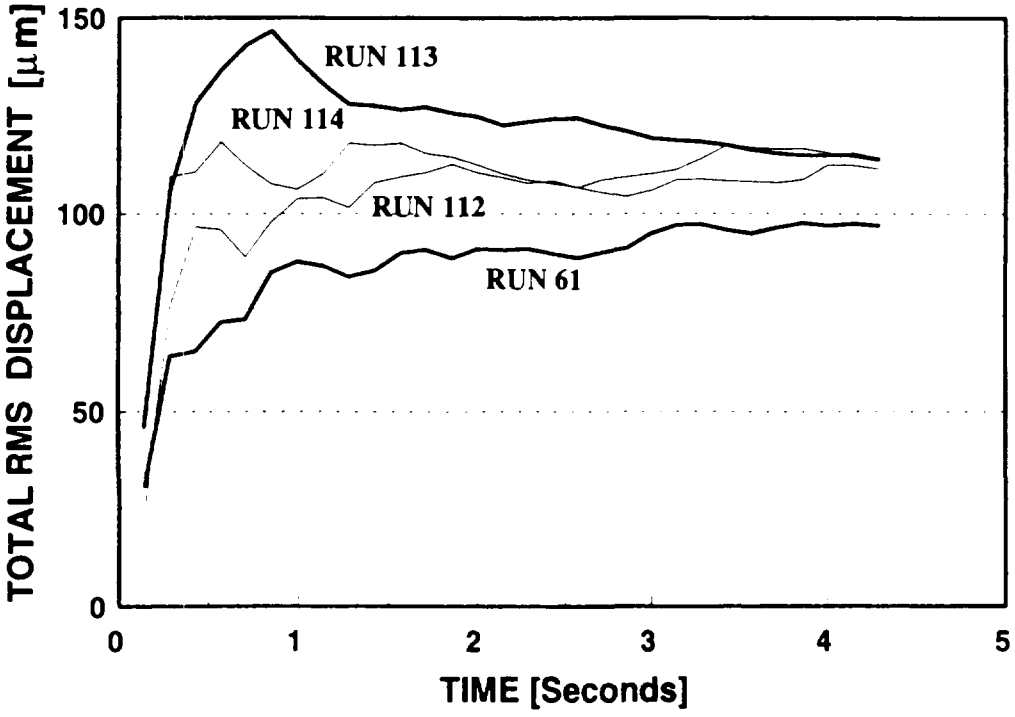

Figure 4: Total Displacements for Random Turbulence Excitation with Different Sets of Random Numbers

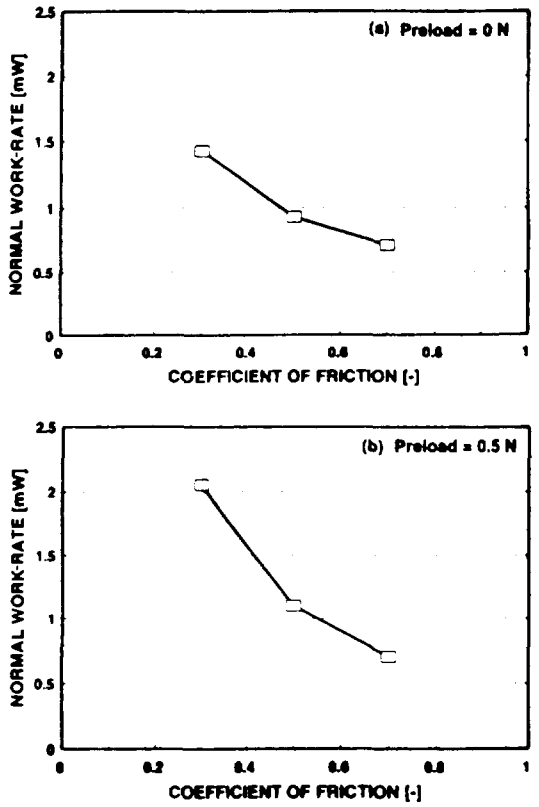

Figure 5: The Effect of Coefficient of Friction on Work-Rate for Turbulence Excitation

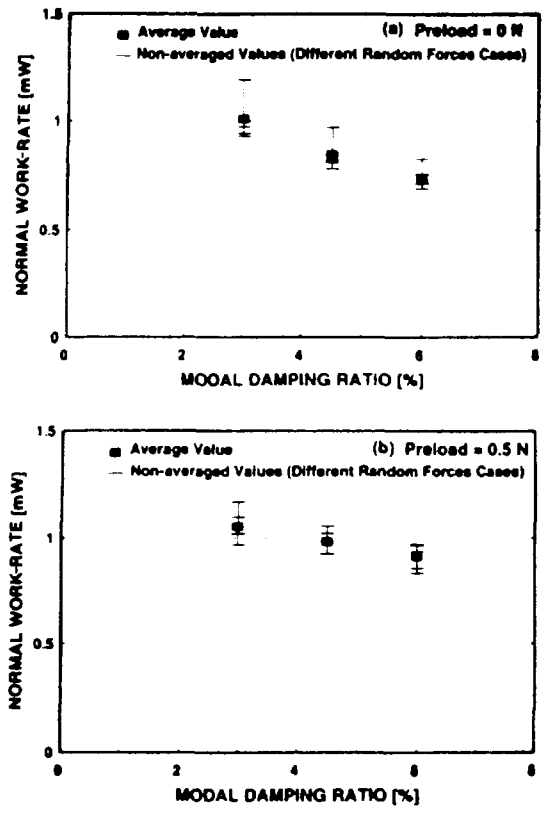

Figure 6: The Effect of Modal Damping Ratio on Work-Rate

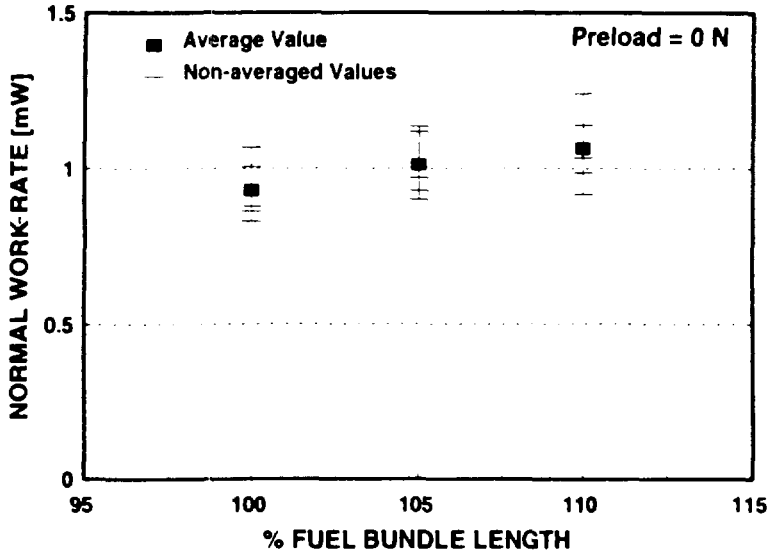

Figure 7: The Effect of Fuel Bundle Length on Work-Rate

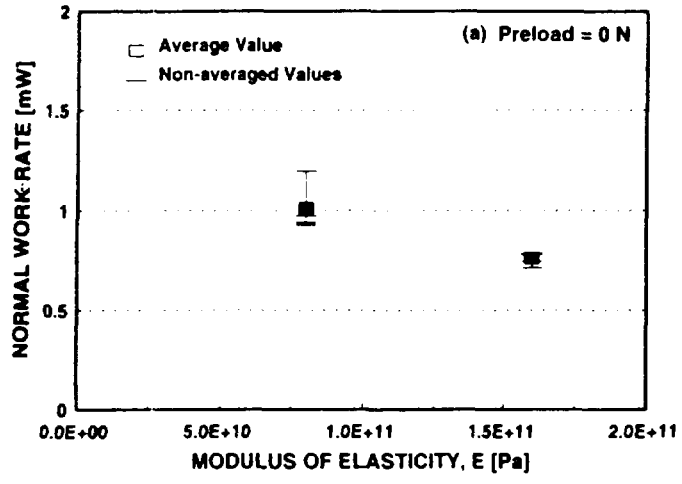

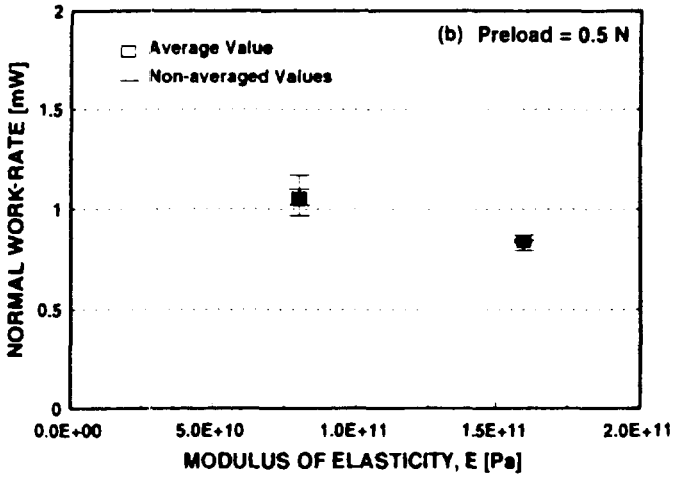

Figure 8: The Effect of Fuel Element Stiffness on Work-Rate

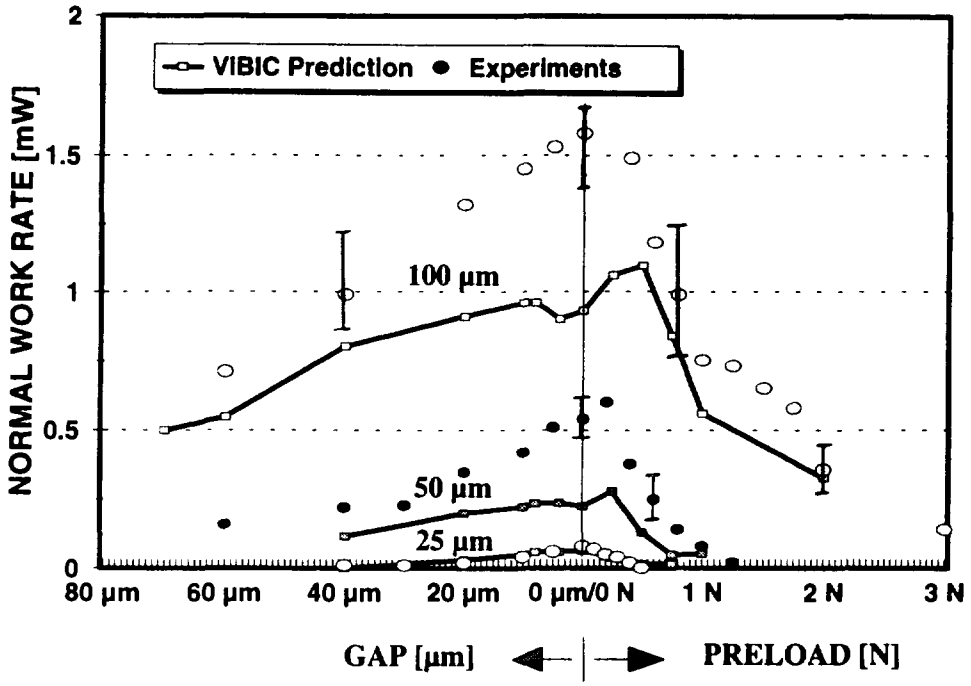

Figure 9: The Effect of Gap/Preload on Work-Rate due to Turbulence Excitation

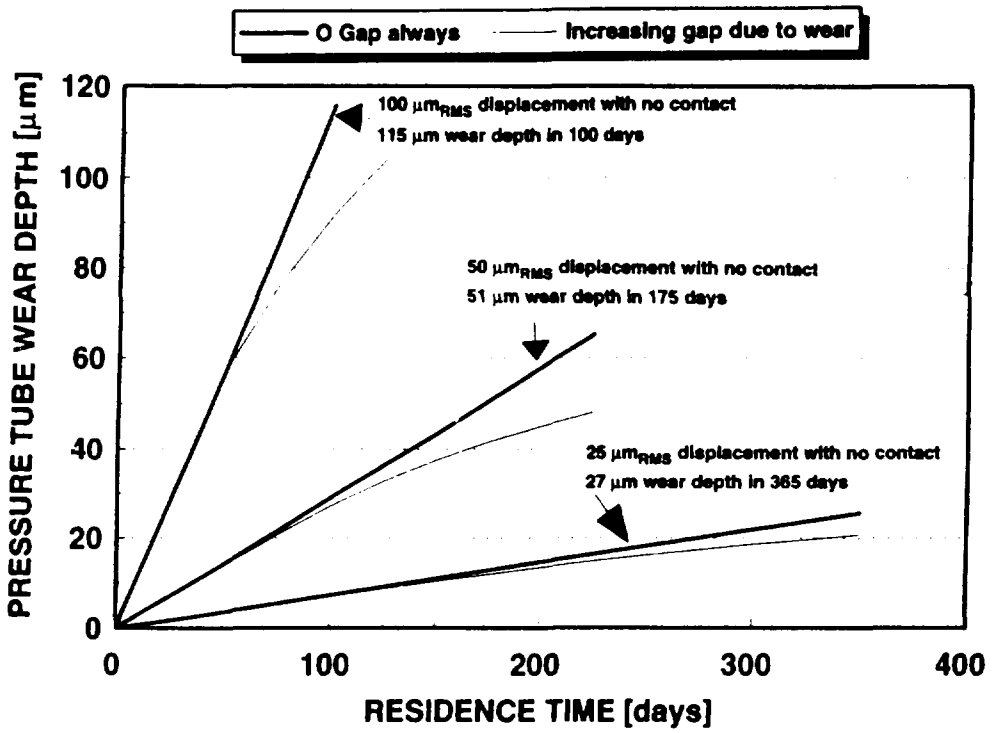

Figure 10: Fretting Damage for Turbulence Excitation

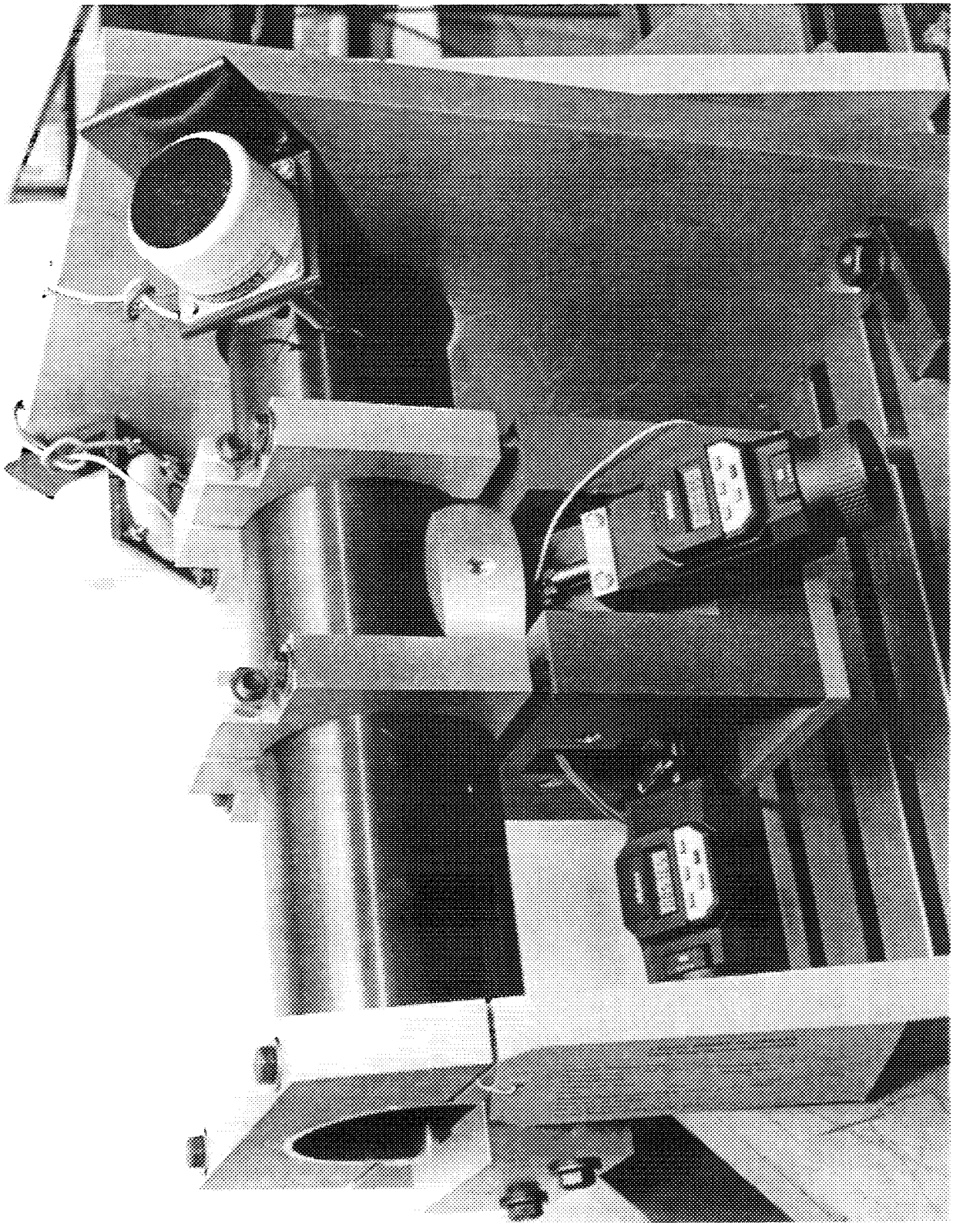

Figure 11: Experimental Setup